ELSEVIER

Contents lists available at ScienceDirect

NeuroImage

journal homepage: www.elsevier.com/locate/neuroimage



Trait self-reflectiveness relates to time-varying dynamics of resting state functional connectivity and underlying structural connectomes: Role of the default mode network



Daouia I. Larabi ^{a,b,c,*,1}, Remco J. Renken ^a, Joana Cabral ^{d,e}, Jan-Bernard C. Marsman ^a, André Aleman ^{a,f}, Branislava Ćurčić-Blake ^a

- ^a University of Groningen, University Medical Center Groningen, Department of Biomedical Sciences of Cells and Systems, Cognitive Neuroscience Center, Groningen, the Netherlands
- b Institute of Neuroscience and Medicine, Brain & Behaviour (INM-7), Research Centre Jülich, Jülich, Germany
- ^c Institute of Systems Neuroscience, Medical Faculty, Heinrich Heine University Düsseldorf, Düsseldorf, Germany
- ^d Department of Psychiatry, University of Oxford, Oxford, United Kingdom
- ² Life and Health Sciences Research Institute, School of Medicine, University of Minho, Braga, Portugal
- ^f University of Groningen, Department of Psychology, Groningen, the Netherlands

ARTICLE INFO

Keywords: Phase synchronization Dynamic functional connectivity Functional networks DTI connectome Gray matter connectome Graph analysis

ABSTRACT

Background: Cognitive insight is defined as the ability to reflect upon oneself (i.e. self-reflectiveness), and to not be overly confident of one's own (incorrect) beliefs (i.e. self-certainty). These abilities are impaired in several disorders, while they are essential for the evaluation and regulation of one's behavior. We hypothesized that cognitive insight is a dynamic process, and therefore examined how it relates to temporal dynamics of resting state functional connectivity (FC) and underlying structural network characteristics in 58 healthy individuals.

Methods: Cognitive insight was measured with the Beck Cognitive Insight Scale. FC characteristics were calculated after obtaining four FC states with leading eigenvector dynamics analysis. Gray matter (GM) and DTI connectomes were based on GM similarity and probabilistic tractography. Structural graph characteristics, such as path length, clustering coefficient, and small-world coefficient, were calculated with the Brain Connectivity Toolbox. FC and structural graph characteristics were correlated with cognitive insight.

Results: Individuals with lower cognitive insight switched more and spent less time in a globally synchronized state. Additionally, individuals with lower self-reflectiveness spent more time in, had a higher probability of, and had a higher chance of switching to a state entailing default mode network (DMN) areas. With lower self-reflectiveness, DTI-connectomes were segregated less (i.e. lower global clustering coefficient) with lower embeddedness of the left angular gyrus specifically (i.e. lower local clustering coefficient).

Conclusions: Our results suggest less stable functional and structural networks in individuals with poorer cognitive insight, specifically self-reflectiveness. An overly present DMN appears to play a key role in poorer self-reflectiveness.

1. Introduction

The ability to reflect upon oneself, to not be overly confident of one's own beliefs and to be open to corrective feedback from others is essential for the evaluation and regulation of one's own behavior, emotions and thoughts. An impairment in this ability has been suggested to play a role

in the impaired ability to recognize one's own symptoms in psychiatric disorders. This has been referred to as "impaired insight into illness", a phenomenon that is seen in several neurological and psychiatric illnesses such as schizophrenia, dementias, substance-related disorders, and obsessive-compulsive disorder (Dam, 2006; Goldstein et al., 2009; Mangone et al., 1991; Matsunaga et al., 2002). Patients with impaired

https://doi.org/10.1016/j.neuroimage.2020.116896

Received 29 January 2020; Received in revised form 15 April 2020; Accepted 27 April 2020 Available online 26 May 2020

^{*} Corresponding author. University of Groningen, University Medical Center Groningen, Department of Biomedical Sciences of Cells and Systems, Cognitive Neuroscience Center, Antonius Deusinglaan 1, 9713, AV Groningen, the Netherlands.

E-mail address: d.larabi@fz-juelich.de (D.I. Larabi).

¹ Present address:Institute of Neuroscience and Medicine, Brain & Behaviour (INM-7), Research Centre Jülich, Wilhelm-Johnen-Strasse, 52428 Jülich, Germany.

insight are often able to recognize symptoms in others but not in themselves, leading to treatment non-adherence and poorer prognosis (Lincoln et al., 2007; Startup, 1997). The abilities to reflect upon oneself (i.e. self-reflectiveness) and to not be overly confident of one's own beliefs (i.e. self-certainty) are collectively termed cognitive insight (Beck et al., 2004). Learning more about the neural substrate of cognitive insight in healthy individuals may help gain a better understanding of impairments and mechanisms underpinning impaired insight and self-reflectiveness in psychiatric and neurological disorders. This could be of value for treatment, as these aberrant cognitive thinking styles can be used as intervention targets.

Thus far, only one functional magnetic resonance imaging (fMRI) study investigated the relationship between cognitive insight and brain activation in *healthy* individuals. The authors found significant positive associations between self-reflectiveness and brain activation in the right ventrolateral prefrontal cortex (VLPFC), and between self-certainty and activation in the midbrain during an external source memory task (Buchy et al., 2014). Several studies have been conducted in *patients with schizophrenia*; significant correlations were found between self-reflectiveness or cognitive insight and activation of several regions distributed across the brain during an external source memory task (Buchy et al., 2015), a reality evaluation and recognition task (Lee et al., 2015) and a self-reflection task (van der Meer et al., 2013). No significant associations were found between brain activation and self-certainty (Buchy et al., 2015; Lee et al., 2015; van der Meer et al., 2013).

It should be noted that the cognitive insight measure was designed to measure the ability to take distance from, reflect upon and re-evaluate one's own beliefs and interpretations. Self-reflectiveness, as it is part of the cognitive insight construct, therefore, is different from self-reflection (van der Meer et al., 2010), self-related or self-referential processing (Northoff et al., 2006; Qin and Northoff, 2011), and self-generated thoughts (Andrews-Hanna et al., 2014) which are considered broader processes involving any kind of self-referential processing. In contrast, cognitive insight refers to very specific conscious reflection on one's own beliefs and interpretations and therefore has a stronger meta-cognitive component. Not surprisingly, there is some conceptual overlap and overlap in associated brain regions, as self-referential processing is mostly associated with cortical midline or default mode network structures such as the medial prefrontal cortex and posterior cingulate cortex, in addition to other areas such as the insula. In contrast, results of previous studies on cognitive insight suggest spatially diffuse abnormalities across the brain in individuals with poorer self-reflectiveness or cognitive insight, which supports the idea that cognitive insight may be dependent on integration of higher-order cognitive functions which cannot be pinpointed to isolated brain areas. Therefore, methods taking the complex network of the brain into account should provide a more meaningful explanation of impaired cognitive insight than a regional approach.

Evidence from fMRI-recordings indicate that BOLD activity of brain areas temporarily synchronizes during the exchange of information (Beckmann et al., 2005; Damoiseaux et al., 2006; De Luca et al., 2006). Moreover, fMRI studies revealed activation of distinct functional networks during resting state when an individual is not engaged in any task (Biswal et al., 1995; Yeo et al., 2011). The relationship between (dynamic) functional networks and cognitive insight has not been studied in healthy individuals thus far. In schizophrenia spectrum disorders, a previous study showed that reduced resting state functional connectivity (FC) in the left inferior frontal cortex in the right dorsal attention network was associated with self-certainty (Gerretsen et al., 2014). This study examined static FC which reflects mean connectivity over the scan session. However, during resting state, the brain spontaneously transitions between different states, characterized by different configurations of FC (i.e. functional networks), which may reflect distinct mental processes (Kucyi et al., 2018). Vidaurre et al. (2019) showed that while static FC appears to be driven by structural differences between individuals (Bijsterbosch et al., 2018; Llera et al., 2019), time-varying functional connectivity uniquely relates to behavioral traits (Vidaurre et al., 2019).

Their results suggest that time-varying FC might reflect transient exchange of information that fluctuates over and above the static FC that was shown to be related to structure (Vidaurre et al., 2019). The authors suggested that these time-varying dynamics of functional connectivity might be especially related to dynamic elements of cognition (Kucyi et al., 2017; Smallwood and Schooler, 2015; Vidaurre et al., 2019). Studies have indeed shown the importance of examining time-varying dynamics of functional connectivity for processes such as social cognition (Sun et al., 2020), self-serving bias (Cui et al., 2020) and attention (Fong et al., 2019). We hypothesize that cognitive insight requires (social/meta-) cognitive processes such as self-monitoring, processing and regulation of one's own state and performance while integrating new information into one's thought processes and re-evaluating one's own beliefs. This dynamic process requires constant updating taking the current situation into account. Dynamic FC analyses reveal how functional networks spontaneously fluctuate over time to get more insight into the neural communication underlying cognitive insight. Therefore, in this study, we examined the relationship between cognitive insight and the occurrence, duration and switching profile of different FC states during resting state fMRI. A previous study using the same methodology to define FC states during resting state fMRI, found that individuals with lower cognitive performance (based on an extensive battery of neuropsychological tests) switched more between states, spent less time in a state characterized by global synchronization, and more time in states involving default mode network (DMN) areas (Cabral et al., 2017). Given the association between cognitive insight and neurocognition (see Nair et al., 2014 for a meta-analysis), we hypothesized that individuals with poorer cognitive insight may similarly switch more between states, spend less time in clearly defined states with strong large-scale connectivity, and spend more time in the DMN-state.

Moreover, even though studies have shown a dependence of FC on anatomical structure (Sporns et al., 2004), structural and functional abnormalities are often contradictory (for example in schizophrenia (Fornito and Bullmore, 2015)). We therefore additionally relate cognitive insight to characterizations of structural networks. DTI connectomes represent anatomical connectivity based on probabilistic tractography on diffusion weighted imaging (DWI). Gray matter (GM) connectomes are based on similarity in GM-structure, which might result from mutual genetic influences (Schmitt et al., 2009), axonal tension (Essen, 1997; Gong et al., 2012; Hilgetag and Barbas, 2005), synchronized developmental change (Alexander-Bloch et al., 2013), or functional coactivation of brain areas (Alexander-Bloch et al., 2013; Evans, 2013; Seeley et al., 2009). Altogether, by investigating the relation between cognitive insight and brain variability measured with different MRI-modalities, we aim to get a more comprehensive view of the neural correlates of cognitive insight.

2. Materials and methods

2.1. Participants

We acquired resting state functional magnetic resonance imaging (rs-fMRI), diffusion weighted imaging (DWI) and structural MRI (sMRI) data of 59 healthy individuals. Participants were recruited in the local community through advertisements and word of mouth. Participants were selected from a larger sample of 200 participants based on the distribution of their scores on the self-reflectiveness subscale of the Beck Cognitive Insight Scale (BCIS) (Beck et al., 2004). We created three groups (i.e. with 25% lowest, 50% average and 25% highest self-reflectiveness scores) and randomly selected 20 individuals from each group. Groups were matched on sex, age, and education. Inclusion criteria were: right-handedness (i.e. score>60 on Edinburgh Handedness Inventory) (Oldfield, 1971), age between 18 and 65, normal or corrected to normal vision, MRI-compatibility, capability of giving informed consent and fluency in written and spoken Dutch language. Exclusion criteria were epilepsy or family history of epilepsy, use of medication that can

influence task performance, recreational drug use, presence or history of neurological, psychiatric or substance dependence disorder, smoking, and a score \geq 41 on the Schizotypal Personality Questionnaire (Raine, 1991). This study was in accordance with the latest version of the Declaration of Helsinki and was approved by the medical ethical board of the University Medical Center Groningen. All participants gave written informed consent prior to participation. One participant was excluded during analyses (see Results section for details), leaving 58 participants for further analyses.

2.2. Self-reflectiveness, self-certainty and cognitive insight

Self-reflectiveness, self-certainty and their combination (i.e. composite index score of cognitive insight; see distribution in Figure S1) were measured with the Beck Cognitive Insight Scale (BCIS) (Beck et al., 2004). The BCIS is a 15-item self-report questionnaire consisting of two subscales measuring individuals' ability to reflect upon themselves (i.e. self-reflectiveness; Figure S2) and their overconfidence in their own beliefs (i.e. self-certainty; Figure S3). Answers are given on a 4-point Likert-scale. A composite index score of cognitive insight is computed by subtracting self-certainty scores from self-reflectiveness scores. Better cognitive insight is reflected by higher composite index and self-reflectiveness scores and lower self-certainty scores (Beck et al., 2004). Two subscale scores and the composite index score were used for (f)MRI-analyses.

Results of previous studies suggest that individuals can reliably rate their experiences (Riggs et al., 2012), given that not only the initial validation study but also several other studies from other groups have shown reliability and validity of the BCIS. The BCIS can distinguish patients with psychosis from patients without psychosis and healthy individuals (Riggs et al., 2012), and several studies showed increased self-certainty (i.e. poorer cognitive insight) in individuals with at-risk mental state (Uchida et al., 2014) or at clinical high risk for psychosis (Kimhy et al., 2014).

2.3. Functional connectivity analyses

2.3.1. Image acquisition

Seven minutes and 47 s (215 timepoints) of resting state BOLD functional scans were acquired using a Siemens MAGNETOM Prisma 3T MRI scanner (Siemens, Erlangen, Germany) with a multi-echo-EPI sequence [TR = 2170 ms; TE = 9.74, 22.1, and 34.46 ms; FA = 60° ; FOV = 224 × 224 mm; matrix size = 75×75 mm; 39 axial slices; voxel size = $3 \times 3 \times 3$ mm; slice order = sequential descending] (Feinberg et al., 2010; Moeller et al., 2010; Xu et al., 2013). Functional scans were acquired with an in-plane acceleration factor (GRAPPA) of 4. Participants were shown a fixation cross, and they were instructed to relax, stay focused on the fixation cross and not fall asleep.

2.3.2. Preprocessing resting state fMRI-data

Since our fMRI-data was acquired at three echo times, data was denoised using meica.py in AFNI (version 2.5 beta9) (Cox, 1996; Kundu et al., 2013, 2012). In short, the following steps were taken: (1) slice time correction, (2) realignment, (3) concatenating all data across echo times and space, (4) identification of components using decomposition of multi-echo data with independent component analysis (ICA), (5) differentiation of BOLD-components from non-BOLD components, (6) removal of non-BOLD components from time series by using them as noise regressors in time course de-noising, and (7) combination of the three denoised echo time series into one denoised single time series using a T2* weighting scheme (Kundu et al., 2012; Posse et al., 1999).

Consequently, denoised timeseries were additionally preprocessed in SPM12 (www.fil.ion.ucl.ac.uk/spm) in Matlab R2015a (Mathworks inc, Natick, MA). Steps included: (1) construction of temporal mean time series, (2) coregistration of all functional images (i.e. source image = mean image created during previous step), and anatomical

image (i.e. reference image) and (3) normalization of all images to MNI space and reslicing of voxels to $2\times2\times2\,\mathrm{mm}^3$ voxels. Last, data was filtered in Matlab with band-pass temporal filtering (0.04–0.07 Hz) using a 7th-order Butterworth filter (Glerean et al., 2012). We then extracted time series for 90 cortical and subcortical areas of the Automated Anatomical Labeling (AAL) atlas (Tzourio-Mazoyer et al., 2002) by averaging the non-zero signal of all voxels within that area. The AAL-atlas was chosen so that results could be compared with previous studies using the same methodology (Cabral et al., 2017; Figueroa et al., 2019; Lord et al., 2019).

2.3.3. Time-varying dynamics of resting state functional connectivity

In order to examine dynamic FC, we used a data-driven method called Leading Eigenvector Dynamics Analysis (LEiDA). The method is described in Cabral et al. (2017), and the code is available on Github (github.com/juanitacabral/LEiDA).

We first estimated the phase of the fMRI time series for each of the 90 brain regions using the Hilbert transform. 14 volumes (i.e. 2*7 because of 7th-order Butterworth filter) at the beginning and ending of scanning were discarded to avoid edge effects that are inherent to the Hilbert transform, leaving 187 time points (i.e. 6 min and 46s) for further analyses. Next, we calculated phase coherence as the cosine of the difference in phases of two regions at each time point. This resulted in a symmetric BOLD phase coherence matrix of size $90 \times 90 \times 187$ for each individual (i.e. 90 brain areas and 187 timepoints). In order to reduce the dimensionality of the functional connectivity patterns per time point, we took the 1x90 leading eigenvector of each BOLD phase coherence matrix, resulting in 10846 leading eigenvectors (i.e. 58 individuals \times 187 time points). A matrix of size 90x10846 was created by concatenating all eigenvectors from all subjects and time points. Kmeans clustering (with 2-20 clusters, each repeated 20 times) was applied on all 10846 leading eigenvectors to get functional states across individuals and time points. The number of clusters with the highest Dunn index was selected (Dunn, 1973). A higher Dunn index indicates better clustering reflected by compact clusters (i.e. small variance within cluster) which are separated well from other near clusters. This resulted in a 58x187 matrix (i.e. subject x time point), with information on which state each time point belonged to. We compared the states to the seven resting-state networks as described by Yeo et al. (2011). The seven resting-state networks were transformed into vectors with 90 elements (i.e. 90 AAL-areas) representing how much that AAL-area contributes to the resting state network (Lord et al., 2019). Correlations were then calculated between the seven networks and states 2-4. Only positive elements were kept of the state-vectors as they represent the areas that formed a network desynchronized from the rest of the brain (Lord et al., 2019).

After obtaining FC states, we calculated the switching frequency (i.e. number of transitions between states per second), probabilities of occurrence (i.e. fraction of time points in one state during entire scan session), lifetime (i.e. mean number of consecutive time points in the same state) and switching profile (i.e. probabilities of switching from a certain state to another) between states (i.e. clusters) per individual (Cabral et al., 2017; Figueroa et al., 2019; Lord et al., 2019; Stark et al., 2019). We then computed associations of these values with our insight measures (see Statistical Analyses).

2.4. Structural DTI connectome analyses

2.4.1. Image acquisition

Diffusion-weighted images were acquired using a Siemens MAGNE-TOM Prisma 3T MRI scanner (Siemens, Erlangen, Germany) with a 64-channel head coil. 60 slices were acquired with the following parameters: $TR = 8500 \, \text{ms}$; $TE = 90 \, \text{ms}$; $FOV = 256 \times 256 \, \text{mm}$; matrix size = $128 \times 128 \, \text{mm}$; image resolution $2 \times 2 \times 2 \, \text{mm}^3$ without gap; GRAPPA = 2, SMS = 2. In total, 74 volumes were acquired per subject, ten without diffusion weighting (b = 0 s/mm2) and 64 with diffusion

weighting (b = 1000 s/mm2) along 64 isotropically distributed directions.

2.4.2. Structural DTI connectome analyses

The following steps were conducted in FSL version 5.0 (Woolrich et al., 2009) with default parameters: (1) correction for eddy-current induced distortion and motion with the eddy tool (Andersson and Sotiropoulos, 2016), (2) skull stripping of the T1-weighted image with the brain extraction tool (BET) (Smith, 2002), (3) fitting the probabilistic diffusion model with BEDPOSTX in the FDT toolbox (Behrens et al., 2007, 2003), (4) (a) coregistration of the T1-image into diffusion space (input = T1, reference = diffusion image), (b) warping of MNI-template diffusion space (input = MNI152_T1_11 mm_brain; ence = T1-image in diffusion space) and (c) warping the AAL-mask to diffusion space with FLIRT (input = AAL-mask; using normalization matrix from FLIRT transformation of MNI-template to diffusion space) (Jenkinson et al., 2002; Jenkinson and Smith, 2001), (5) parcellation into 90 non-cerebellar brain areas with the AAL-atlas, (6) creation of a 90 × 90 network matrix using PROBTRACKX2 (number of samples = 5000; options omatrix1 and network) (Behrens et al., 2007, 2003), and (7) fractional scaling and symmetrizing of the matrix following Donahue et al. (2016). Ultimately, these steps resulted in a 90×90 symmetrically weighted network of streamline probabilities per individual.

Matrices were normalized (i.e. maximum value was scaled to 1; function weight_conversion) using the Brain Connectivity Toolbox (Rubinov and Sporns, 2010). We calculated path length (function distance_wei_floyd with log transform) and clustering coefficient (function clustering_coef_wu_sign with Zhang & Horvath formula). In addition, 20 randomized reference networks with preserved weight, degree and strength distributions were created per individual (function null_model_und_sign), and their higher-order graph metrics were calculated. Subsequently, we calculated normalized path length and normalized clustering coefficient by dividing path length and clustering coefficient of each network, respectively, by those averaged from 20 random networks. Last, we computed small-world coefficients by dividing normalized clustering coefficient with normalized path length.

2.5. Structural gray matter connectome analyses

2.5.1. Image acquisition

Structural scans were acquired in the sagittal plane using a Siemens MAGNETOM Prisma 3T MRI scanner (Siemens, Erlangen, Germany). A Magnetization Prepared Rapid Gradient Echo (MPRAGE) sequence was used with the following parameters: voxel size = $1\times1\times1.2$ mm; FOV = $176\times240\times256$ mm; TR = 2300 ms, TE = 2.98 ms; TI = 900 ms; FA = 9° .

2.5.2. Structural gray matter connectome analyses

The method for construction of gray matter networks is described in Tijms et al. (2012) (Tijms et al., 2012) and the code is available on Github (https://github.com/bettytijms/Single_Subject_Grey_Matter_Networks). In short, gray matter segmentations were parcellated into cubes, each consisting of 27 voxels (3 \times 3 \times 3 voxels). Values within these cubes were correlated with each other to create a N \times N similarity matrix. The maximum correlation between two cubes was computed by calculating correlations between cubes while rotating the seed cube with multiples of 45°. Each network was binarized by applying a subject-specific threshold of p < 0.05, as determined by permutation testing.

An AAL-atlas was warped to subject space per individual with (1) inverse deformation parameters obtained during segmentation and (2) coregistration parameters obtained during creation of gray matter networks. Global graph metrics were calculated per individual using the Brain Connectivity Toolbox while only including nodes (i.e., cubes) of which at least one voxel fell within the AAL-mask. We calculated basic metrics such as degree (i.e. number of edges; function degrees_und) and

density (i.e. number of existing edges relative to number of all possible edges; function density_und), and higher-order metrics such as path length (i.e. the minimum number of edges between any two nodes; functions distance_bin and charpath) and clustering coefficient (fraction of node's neighbors that are each other's neighbors; function clustering_coef_bu). In addition, 20 randomized reference networks with identical size, degree and degree distribution were created per individual (function randmio_und) and their higher-order graph metrics were calculated using the Brain Connectivity Toolbox. Last, normalized path length, normalized clustering coefficient and small-world coefficients were calculated.

2.6. Covariates

All behavioral data was analyzed in R version 3.5.2 (R Core team, 2018). Matching of groups on sex was checked with ANOVA, while matching on age and education was checked with Spearman correlations between these variables and cognitive insight (i.e., self-reflectiveness, self-certainty or composite index scores). We additionally checked the differences in cognitive insight between individuals with and without experience with mindfulness or meditation. The correlation between cognitive insight and motion during resting state fMRI was investigated after calculating framewise displacement (Power et al., 2012) on motion parameters obtained from realignment during ME-ICA (see Figure S4 for mean framewise placement per participant). With regard to structural connectome analyses, earlier studies showed that basic graph metrics influence higher-order graph metrics (van Wijk et al., 2010). Therefore, we checked (Spearman) correlations between cognitive insight (i.e., self-reflectiveness, self-certainty or composite index scores) and size, degree and density of gray matter connectomes. We did not correlate cognitive insight with the size, degree and density of DTI connectomes, because these values were identical across subjects (i.e., size = 90, degree = 89, density = 100%). Lastly, given the wide age range of participants and variation of resting-state networks across age (e.g. Andrews-Hanna et al., 2007), we examined Spearman correlations between age and all functional and structural brain measures.

2.7. Statistical analyses

The relationship between cognitive insight and time-varying dynamics of resting state fMRI was examined with Spearman correlations between self-reflectiveness, self-certainty or the composite index score of cognitive insight on one hand, and state metrics (i.e. switching frequency, lifetime of states, occurrence of being in certain states) on the other hand. In case of significant correlations, we additionally investigated the probabilities of switching from a certain state to another for states that were significantly related to cognitive insight in prior analyses.

The relationship between cognitive insight and structural connectome organization was assessed using (partial) Spearman correlations between self-reflectiveness, self-certainty or cognitive insight and higher-order graph metrics (i.e. path length, clustering coefficient and small-world coefficients) for both the gray matter as well as the DTI connectomes. In case of gray matter connectomes, we corrected for total gray matter volume.

In line with previous studies applying the same methodology, findings were considered significant at a threshold of p < 0.05, two-tailed. As this is the first multimodal investigation of cognitive insight and we wanted to enhance the probability of hypothesis-generating findings at this early stage of investigation, we additionally report trend-level significant results (p-value between 0.05 and 0.1) in Tables 3–4 and Fig. 6 (but not in the main text of the Results section). The raw data is available by contacting the corresponding author.

3. Results

3.1. Participants

Our study included 59 participants. One participant was excluded because of no convergence of the ME-ICA algorithm on their fMRI-data. All characteristics of the remaining 58 participants can be seen in Table 1.

3.2. Covariates

No significant correlations were found between cognitive insight (i.e., self-reflectiveness, self-certainty or composite index score) and either age, education, or motion during resting state fMRI, nor size or degree of gray matter connectomes (see Table S2). No significant differences in cognitive insight were found between males and females, and between individuals with and without experience with mindfulness or meditation. A significant correlation was found between BCIS composite index scores and density of gray matter connectomes. Therefore, density was included as a covariate in further analyses including the BCIS composite index score. Lastly, significant correlations were found between age and normalized clustering coefficient, normalized path length, and smallworld coefficient of GM networks (see Table S3). Therefore, further analyses with these variables were additionally controlled for age. No significant correlations were found between age and time-varying dynamics of resting state functional connectivity, nor between age and DTI connectome characteristics.

3.3. Time-varying dynamics of resting state functional connectivity

K-means clustering revealed an optimal solution with four clusters, in which each cluster represents a recurrent state of FC (Figure S5). The states are represented by a 90×4 matrix (i.e. ROI x state) reflecting the

Table 1 Participant characteristics (n = 58).

| | Mean (SD) |
|---|------------------|
| Sex (number of males/females) | 14/44 |
| Age (years) | 25 (10.33) |
| Education level ^a | 6.01 (0.40) |
| Mindfulness/meditation experience (number yes/no) | 13/45 |
| Insight Orientation Scale (IOS) | 25 (3.38) |
| Beck Cognitive Insight Scale (BCIS) | |
| Self-reflectiveness | 10.66 (3.32) |
| Self-certainty | 6.52 (2.38) |
| Composite index | 4.14 (4.63) |
| Kentucky Inventory of Mindfulness Skills (KIMS) | |
| Observing | 38.16 (7.28) |
| Describing | 28.98 (4.71) |
| Acting with awareness | 31.29 (4.20) |
| Accepting without judgement | 35.52 (5.52) |
| Total | 133.95 (11.16) |
| Ten Item Personality Inventory (TIPI) | |
| Openness to experience | 10.64 (2.40) |
| Conscientiousness | 10.09 (2.14) |
| Extraversion | 9.52 (2.77) |
| Agreeableness | 11.24 (1.56) |
| Emotional stability | 10.60 (2.17) |
| QIDS-SR depressive symptoms | 2.90 (1.83) |
| Intelligence quotient ^b | 97.22 (9.70) |
| Processing speed ^c | 67.71 (11.26) |
| Gray matter connectomes | |
| Gray matter volume | 560.17 (52.01) |
| Network size | 5578.09 (475.73) |
| Network degree | 1019.97 (106.75) |
| Network density | 0.18 (0.009) |

 $\label{eq:Abbreviations: QIDS-SR = Quick Inventory of Depressive Symptomatology-Self-Report.$

contribution of each brain area to each state. Additionally, we had a 58 x 187 matrix (i.e. subject x time point) with information on which state each time point belonged to. State 1 (occurring about 52% of the time) reflects a state of global BOLD coherence in line with previous studies examining resting state functional connectivity states (Cabral et al., 2017; Lord et al., 2019). During the other states, BOLD phases of a limited set of regions desynchronize with BOLD phases of the rest of the brain (while retaining synchrony amongst themselves) thereby forming a network (Fig. 1). State 2, occurring 19% of the time, represents a network consisting of areas such as the Rolandic operculum, insula, supramarginal gyrus, putamen, right pallidum, left thalamus, Heschl gyrus, left superior temporal gyrus and left amygdala. This network correlated with the ventral attention network of Yeo et al. (2011) (r = 0.5, p < 0.001; Figs. 1-2 and Table 2). State 3 represents a network consisting of areas such as the medial superior frontal gyrus, medial orbitofrontal gyrus, gyrus rectus, left olfactory gyrus, left inferior orbitofrontal gyrus, anterior cingulate cortex, posterior cingulate cortex, angular gyrus, temporal pole, left middle temporal gyrus. This network, occurring 17% of the time, correlated with the default mode network of Yeo et al. (2011) (r = 0.37, p < 0.001; Figs. 1-2 and Table 2). State 4 represents a network consisting of areas such as calcarine, cuneus, lingual gyrus, superior occipital gyrus, middle occipital gyrus, inferior occipital gyrus, fusiform gyrus and right superior parietal gyrus (probability of occurrence: 12%). This network correlated with the visual network of Yeo et al. (2011) (r = 0.92, p < 0.001; Figs. 1-2 and Table 2). Thus, states 2-4 were significantly positively correlated to only one of the known networks (see Table 2) (Yeo et al., 2011). Therefore, in the rest of the text, these states will be addressed with the name of the known network (Yeo et al., 2011).

3.4. Statistical analyses

3.4.1. Cognitive insight and time-varying dynamics of resting state fMRI

We found that individuals with lower cognitive insight (composite index score) switch more frequently between states ($r_s=-0.28$, p=0.04; Fig. 3A) and have a lower lifetime of the global synchronization state ($r_s=0.26$, p=0.045; Fig. 3B). Similarly, for the self-reflectiveness dimension, individuals with lower self-reflectiveness also switched more between states ($r_s=-0.32$, p=0.01; Fig. 4A). Additionally, they have a higher lifetime ($r_s=-0.27$, p=0.04; Fig. 4B) and a higher probability of occurrence of the DMN-state ($r_s=-0.40$, p=0.002; Fig. 4C). Based on these results, we examined how self-reflectiveness relates to switching probabilities from and towards the DMN-state. We found that individuals with lower self-reflectiveness had a higher chance of switching from the ventral attention network state to the DMN-state ($r_s=-0.32$, p=0.01; Fig. 4D). The other switching probabilities between states and how they relate to cognitive insight are reported in Table 3.

3.4.2. Cognitive insight and structural connectomes

We found a significant correlation between lower self-reflectiveness and lower normalized clustering coefficient of the DTI-connectomes ($r_s = 0.27$, p = 0.04; Fig. 5). No significant associations were observed between cognitive insight and global graph metrics of gray matter connectomes (Table 4).

3.5. Post-hoc analyses of self-reflectiveness and local structural network metrics of the DMN

Given the significant associations that were found between self-reflectiveness and time-varying dynamics of the DMN-state, we calculated Spearman correlations between self-reflectiveness and local structural graph metrics of the 17 areas involved in that state (i.e. all areas with positive weights in state vector reflecting the contribution of AAL-areas to that state). False Discovery Rate (FDR)-correction for multiple testing was applied with the p.adjust function in R (i.e. 17 tests).

For the higher-order graph metrics of the DTI-connectome, we found

^a Based on Verhage (1964).

^b Measured with the Dutch Adult Reading Test (1995).

^c Measured with the digit symbol substitution test.

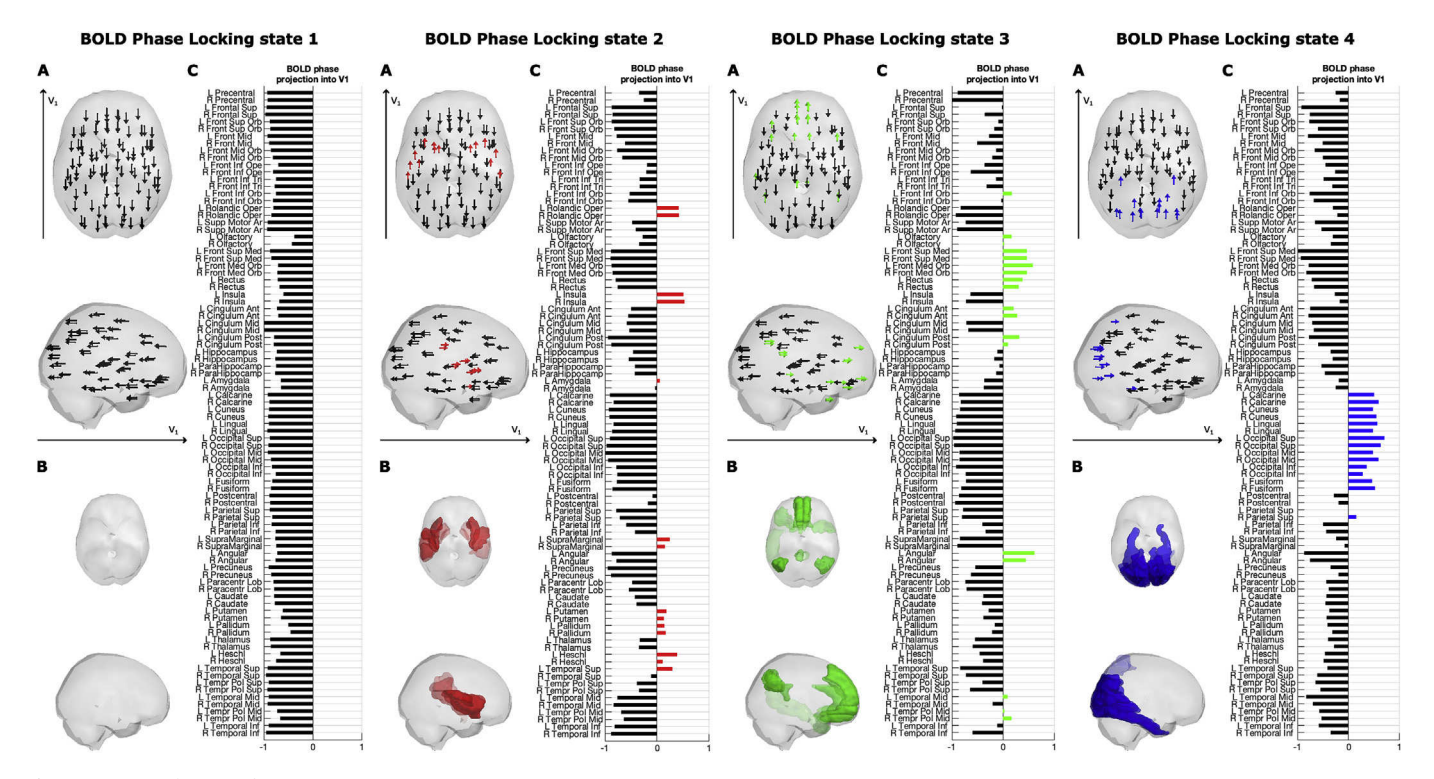


Fig. 1. Dynamic functional connectivity states.

The optimal solution with 4 clusters returns 4 cluster centroids, with size 1x90, each representing the eigenvector of a phase coherence matrix. Each element in the eigenvector corresponds to a brain area in the AAL parcellation, and areas can be divided into communities according to their sign in the eigenvector. A: full unthresholded maps in which the BOLD signal phases in the leading eigenvector V_1 are represented as arrows placed at the center of each AAL-region. In black: projecting in the main (negative) direction of V_1 ; in color: projecting to the opposite (positive) direction of V_1 indicating a phase-shift from the main direction. B: phase-shifted areas are rendered as patches. C: contribution of brain areas to each state. Red: ventral attention network state; Green: default mode network state; Blue: visual network state.

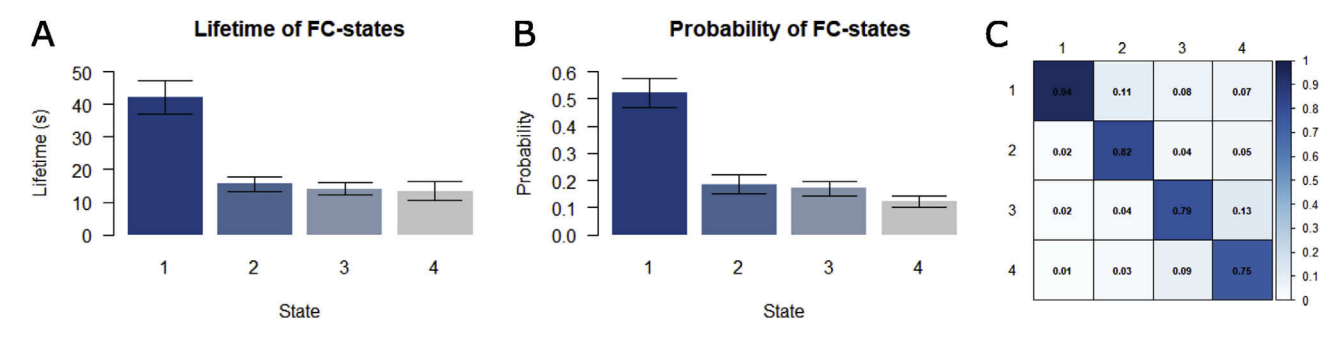


Fig. 2. (A) Lifetime and (B) probability of occurrence of, and (C) switching profile between four functional connectivity states.

Table 2Correlations between states 2–4 and seven resting state networks of Yeo et al. (2011).

| State | Dorsal attention network | Default mode network | Frontoparietal network | Ventral attention network | Limbic network | Somatomotor network | Visual network |
|----------|---|--|--|---|--|--|---|
| #2 | r = -0.16, p = 0.13 | r = -0.19, p = 0.08 | r = -0.13, p = 0.24 | $r = 0.50, p < 0.001 ^{\star}$ | r = -0.17, p = 0.10 | r = 0.11, p = 0.31 | r = -0.16, p = 0.14 |
| #3 #4 | $\begin{aligned} r &= -0.18, p = 0.09 \\ r &= 0.00, p = 0.99 \end{aligned}$ | $\begin{aligned} r &= 0.37^*, p < 0.001 \\ r &= -0.21, p = 0.05 \end{aligned}$ | $\begin{array}{l} r = -0.1, p = 0.37 \\ r = -0.18, p = 0.09 \end{array}$ | $\begin{array}{l} r=-0.19, p=0.08 \\ r=-0.23, p=0.03 \end{array}$ | r = 0.07, p = 0.55 r = -0.03, p = 0.79 | $\begin{aligned} r &= -0.17, p = 0.12 \\ r &= -0.18, p = 0.09 \end{aligned}$ | $\begin{split} r &= -0.18, p = 0.09 \\ r &= 0.92, p < \\ 0.001^* \end{split}$ |

NB: negative correlations indicate that states correlate negatively (i.e. anticorrelate) with the networks of Yeo et al. (2011).

a significant correlation between self-reflectiveness and normalized clustering coefficient of the left angular gyrus ($r_s = 0.43$, p < 0.001, $p_{FDR} = 0.01$; Supplementary Figure S6). No associations between self-reflectiveness and local gray matter connectome characteristics survived the corrected significance threshold (Table 4).

3.6. Post-hoc analyses linking function and structure

Given the significant relationships that were found between cognitive insight on the one hand, and characteristics of dynamic FC or structural connectomes on the other hand (see Fig. 6), we further investigated the

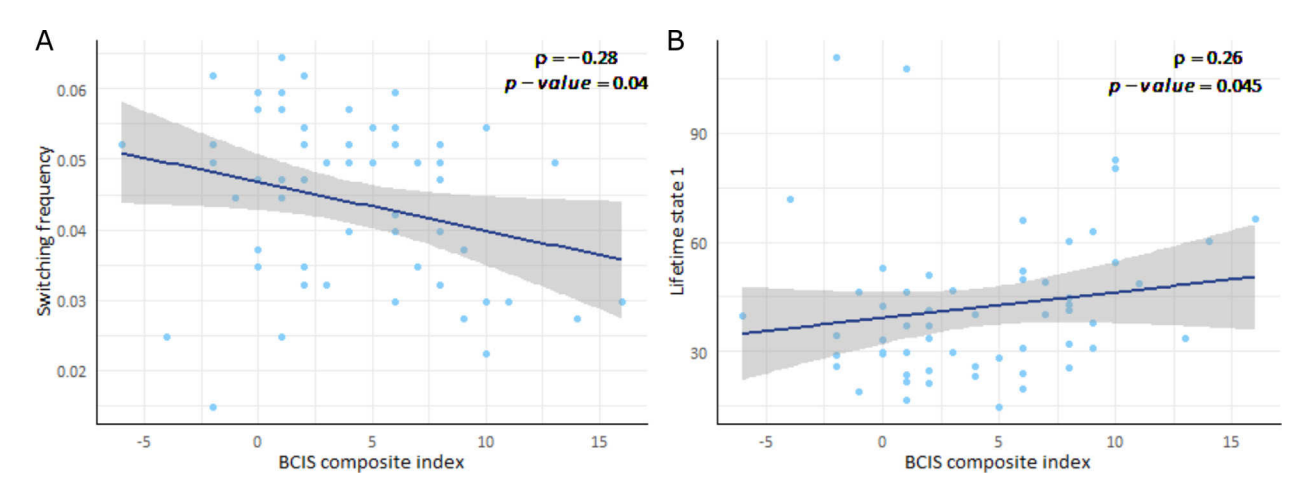


Fig. 3. Scatterplots of Spearman correlations between time-varying dynamics of resting state functional connectivity and BCIS composite index scores.

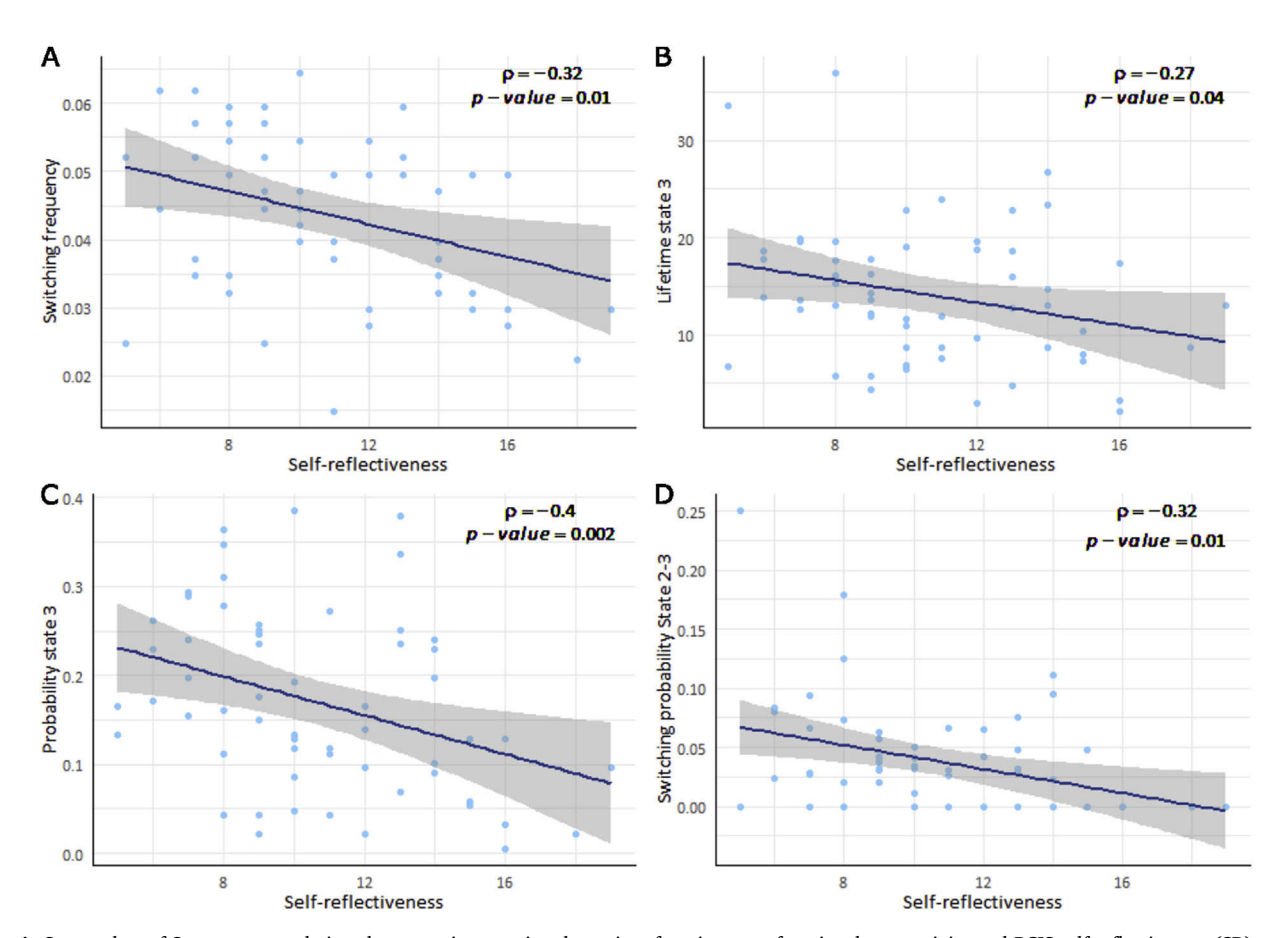


Fig. 4. Scatterplots of Spearman correlations between time-varying dynamics of resting state functional connectivity and BCIS self-reflectiveness (SR) scores.

relationship between function and structure for all relationships shown in Fig. 6.

For the DTI connectome, significant correlations were found between global normalized clustering coefficient and both the switching frequency ($r_s = -0.30$, p = 0.02; Figure S7) and the probability of occurrence of the DMN-state ($r_s = -0.26$, p = 0.046; Figure S8). Furthermore, we found a relationship between lower global small-world coefficient and higher switching frequency ($r_s = -0.32$, p = 0.02; Figure S9). Last, we found that a lower small-world coefficient of the left angular gyrus was related to higher lifetime of the DMN-state ($r_s = -0.26$, p = 0.049; Figure S10) and to a higher probability of occurrence of the DMN-state ($r_s = -0.37$, p = 0.004; Figure S11).

For the gray matter connectome, significant correlations were found between normalized path length of the right temporal pole and lifetime ($r_s = 0.28, \ p = 0.036$; Figure S12) and probability of occurrence ($r_s = 0.31, \ p = 0.02$; Figure S13) of the DMN-state. No significant correlations were found between global path length and function (Fig. 6).

3.7. Robustness and generalizability of results

We tested the robustness and generalizability of the results, by testing the effect of choosing k=3 and k=5 states. The alternative clustering solutions resulted in states that are less separated into and comparable to known functional networks compared to the k=4 solution (Tables S4

Table 3Spearman correlations between cognitive insight and time-varying dynamics.

| | Mean (SD) | BCIS SR | BCIS SC | BCIS CI |
|----------------|--------------|-----------------------------|-----------------|-----------------------------|
| Switching | 0.04 | r _s = -0.32, p = | $r_s = 0.12$, | r _s = -0.28, p = |
| frequency | (0.01) | 0.01* | p = 0.38 | 0.04* |
| Lifetime | | | | |
| State 1 | 42.07 | $r_s = 0.24, p =$ | $r_s = -0.18$, | $r_s = 0.26, p =$ |
| | (20.10) | 0.07 | p = 0.18 | 0.045* |
| State 2 | 15.57 | $r_s = 0.15$, | $r_s = 0.03$, | $r_s = 0.10$, |
| | (8.68) | p = 0.25 | p = 0.80 | p = 0.45 |
| State 3 | 14.08 | $r_s = -0.27, p =$ | $r_s = -0.16$, | $r_s = -0.09$, |
| | (7.11) | 0.04* | p = 0.23 | p = 0.48 |
| State 4 | 13.37 | $r_s = -0.05$, | $r_s = 0.02$, | $r_s = -0.02$ |
| | (11.45) | p = 0.74 | p = 0.91 | p = 0.88 |
| Probability of | occurrence | • | • | • |
| State 1 | 0.52 | $r_s = 0.16$, | $r_s = -0.11$, | $r_s = 0.16$, |
| | (0.21) | p = 0.22 | p = 0.42 | p = 0.23 |
| State 2 | 0.19 | $r_s = -0.01$, | $r_s = 0.10$, | $r_s = -0.06$ |
| | (0.14) | p = 0.93 | p = 0.45 | p = 0.65 |
| State 3 | 0.17 | $r_s = -0.40, p =$ | $r_s = -0.07$, | $r_s = -0.23, p =$ |
| | (0.10) | 0.002* | p = 0.62 | 0.08 |
| State 4 | 0.12 | $r_s = -0.13$, | $r_s = 0.08$, | $r_s = -0.11$, |
| | (0.08) | p = 0.33 | p = 0.57 | p = 0.43 |
| Switching prob | | F | F | P |
| State 1-1 | 0.94 | $r_s = 0.19$, | $r_s = -0.22$, | $r_s = 0.24$ |
| | (0.03) | p = 0.15 | p = 0.11 | p = 0.06 |
| State 1-2 | 0.02 | $r_s = -0.04$ | $r_s = 0.03$, | $r_s = -0.05$, |
| | (0.02) | p = 0.77 | p = 0.82 | p = 0.74 |
| State 1-3 | 0.02 | $r_s = -0.17$, | $r_s = 0.07$, | $r_s = -0.16$, |
| | (0.01) | p = 0.21 | p = 0.63 | p = 0.24 |
| State 1-4 | 0.01 | $r_s = -0.15$, | $r_s = 0.27$, | $r_s = -0.23, p =$ |
| | (0.02) | p = 0.27 | p = 0.04 | 0.08 |
| State 2-1 | 0.11 | $r_s = 0.05$, | $r_s = -0.13,$ | $r_s = 0.08$, |
| | (0.16) | p = 0.70 | p = 0.35 | p = 0.55 |
| State 2-2 | 0.82 | $r_s = 0.09$, | $r_s = 0.12$, | $r_s = 0.01$, |
| | (0.15) | p = 0.50 | p = 0.38 | p = 0.93 |
| State 2-3 | 0.04 | $r_s = -0.32, p =$ | $r_s = 0.06$, | $r_s = -0.24$, |
| otate 2 o | (0.05) | 0.01* | p = 0.65 | p = 0.07 |
| State 2-4 | 0.04 | $r_s = -0.05$, | $r_s = -0.06$, | $r_s = 0.01$, |
| | (0.05) | p = 0.74 | p = 0.65 | p = 0.95 |
| State 3-1 | 0.08 | $r_s = 0.10$, | $r_s = 0.04$ | $r_s = 0.05$, |
| | (0.07) | p = 0.44 | p = 0.73 | p = 0.72 |
| State 3-2 | 0.04 | $r_s = -0.15$, | $r_s = -0.003$ | $r_s = -0.10,$ |
| State o 2 | (0.05) | p = 0.28 | p = 0.98 | p = 0.44 |
| State 3-3 | 0.79 | $r_s = -0.21$, | $r_s = -0.14$, | $r_s = -0.06$, |
| | (0.17) | p = 0.12 | p = 0.31 | p = 0.67 |
| State 3-4 | 0.09 | $r_s = 0.07$, | $r_s = -0.01$, | $r_s = 0.05$, |
| | (0.16) | p = 0.61 | p = 0.94 | p = 0.71 |
| State 4-1 | 0.07 | $r_s = 0.09$, | $r_s = -0.02$ | $r_s = 0.07$, |
| otate 11 | (0.07) | p = 0.51 | p = 0.89 | p = 0.59 |
| State 4-2 | 0.05 | $r_s = -0.06$, | $r_s = 0.09$ | $r_s = -0.07$ |
| June 12 | (0.07) | p = 0.68 | p = 0.53 | p = 0.63 |
| State 4-3 | 0.13 | $r_s = -0.04$ | $r_s = -0.03$ | $r_s = -0.03$ |
| J 10 | (0.17) | p = 0.75 | p = 0.85 | p = 0.81 |
| State 4-4 | 0.75 | $r_s = -0.02$, | $r_s = 0.03$ | $r_s = -0.02$, |
| J | (0.19) | p = 0.86 | p = 0.80 | p = 0.87 |

^{*}Significant at p < 0.05.

Abbreviations: BCIS=Beck Cognitive Insight Scale; SR = self-reflectiveness subscale; SC = self-certainty subscale; CI = composite index score.

Note: state 1 = global synchronization state; state 2 = ventral attention network state; state 3 = default mode network state; state 4 = visual network state.

and S5; Fig. S14 and S15). We also checked whether results changed with these different clustering solutions. Both alternative clustering solutions yielded similar correlations between cognitive insight and time-varying dynamics of resting state functional connectivity. For the k=3 solution, we observed that correlations between self-reflectiveness and lifetime and probability of occurrence of state 1 became larger, while correlations between self-reflectiveness and lifetime of state 3 became smaller, compared to the k=4 solution (Table S6). In the k=3 solution, participants also spent more time in state 1, so this state might entail regions that were allocated to the other states, such as the DMN-state, in the k=4 solution. The k=5 solution also gave similar results (Table S7), with some correlations being slightly smaller. Altogether, findings for

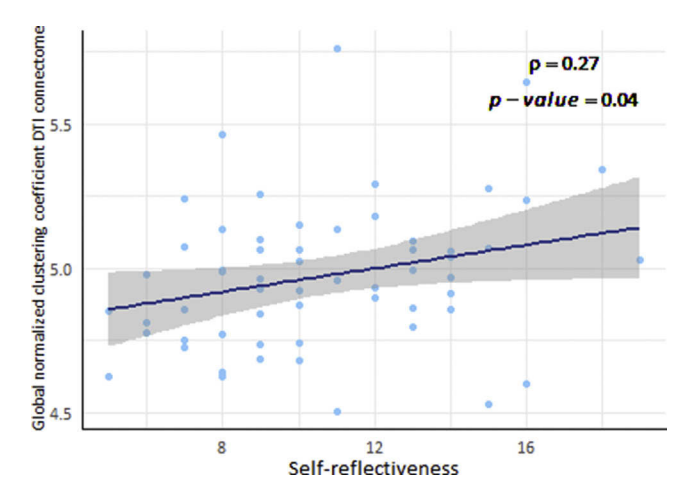


Fig. 5. Scatterplot of Spearman correlation between normalized clustering coefficient of the DTI connectome and BCIS self-reflectiveness (SR) scores.

k=3 and k=5 solutions were similar to the k=4 solution showing that these results are robust across different number of states (see Supplementary Materials for more details).

4. Discussion

In this study, we examined how cognitive insight in healthy individuals relates to dynamic properties of brain *functional connectivity* (assessed with fMRI) and graph properties of the underlying *structural connectomes* (assessed from DTI and gray matter connectivity). We found that individuals with poorer cognitive insight have less stable functional as well as structural networks. This holds specifically for individuals with poorer self-reflectiveness. Furthermore, an overly present DMN appears to play a key role in poorer self-reflectiveness.

4.1. Functional connectivity

Individuals with lower cognitive insight (i.e. composite index score), and self-reflectiveness specifically, switch more between states, suggesting less stable networks. Additionally, they spend less time in a global synchronization state. This state likely reflects the global signal, which is expected to be a combination of neural and non-neural signal (i.e. breathing, motion, changes in vigilance and arousal etc.) (Cabral et al., 2017; Figueroa et al., 2019; Keller et al., 2013; Murphy and Fox, 2017; Scholvinck et al., 2010). It has been suggested to reflect a baseline FC state in which the whole brain is synchronized (Cabral et al., 2017; Figueroa et al., 2019). Lord et al. (2018) indeed showed higher probability of occurrence of the global synchronization state, suggesting a highly integrated brain, after psychedelic drug injection (Lord et al., 2019). This state is costly in energetic terms, and, depending on circumstances, the brain may move efficiently from this globally synchronized baseline state to less energetically costly segregated specialized networks (Figueroa et al., 2019; Nomi et al., 2017).

Furthermore, individuals with lower self-reflectiveness spend more time in and had a higher occurrence of a state characterized by desynchronization of regions implicated in the DMN. The DMN has been suggested to be involved in introspective cognitive functions including mind-wandering (Christoff et al., 2009; Mason et al., 2007). The relationship between cognitive insight and resting state connectivity had not been studied in *healthy individuals* thus far, and a study in *patients with schizophrenia* did not find relationships with the cognitive insight score nor self-reflectiveness dimension (Gerretsen et al., 2014). This study examined static FC, however, while it has been increasingly suggested that transitions between neurocognitive states are important for neurocognitive processes. fMRI-studies did implicate DMN-abnormalities in poorer *cognitive insight*, or *self-reflectiveness* specifically (Buchy et al.,

Table 4Spearman correlations between cognitive insight and global and local (i.e. regions of State 3) graph metrics of structural connectomes.

| | Mean (SD) | BCIS SR | BCIS SC | BCIS CI | | |
|---------------------------|--------------------------------------|--------------------------|-------------------|------------------|--|--|
| Global | | | | | | |
| Gray matter connec | Gray matter connectomes ^a | | | | | |
| Path length | 1.96 | $r_s =$ -0.24, $p =$ | $r_s = 0.08$, | $r_s = -0.24, p$ | | |
| | (0.02) | 0.068 | p = 0.53 | $= 0.077^{b}$ | | |
| Clustering | 0.48 | $r_s = 0.19$, | $r_s = -0.18$, | $r_s = 0.26, p$ | | |
| coefficient | (0.02) | p = 0.15 | p = 0.19 | $=0.056^{b}$ | | |
| Normalized path | 1.08 | $r_s = -0.17$, | $r_s = 0.02,$ | $r_s = -0.14$, | | |
| length | (0.01) | p = 0.20 | p = 0.89 | p = 0.30 | | |
| Normalized | 1.63 | $r_s = -0.09$, | $r_{s} = -0.06$, | $r_s = -0.06$, | | |
| clustering coefficient | (0.06) | p = 0.52 | p = 0.69 | p = 0.66 | | |
| Small-world | 1.51 | $r_s = -0.09$, | $r_s = -0.07$, | $r_s = -0.03$, | | |
| coefficient | (0.02) | p = 0.49 | p = 0.62 | p = 0.81 | | |
| DTI connectomes | | | | | | |
| Path length | 3.55 | r = 0.12, | $r_s = 0.06$, | $r_s = 0.06$, | | |
| | (0.27) | p = 0.3665 | p = 0.63 | p = 0.63 | | |
| Clustering | 0.14 | $r_s = -0.04$, | $r_s = -0.14$, | $r_s = 0.03$, | | |
| coefficient | (0.008) | p = 0.80 | p = 0.31 | p = 0.81 | | |
| Normalized path | 1.39 | $r_s = 0.19$, | $r_s = -0.05$, | $r_s = 0.18$, | | |
| length | (0.02) | p = 0.15 | p = 0.72 | p = 0.19 | | |
| Normalized | 4.97 | $r_s = 0.27, p =$ | $r_s = -0.04$, | $r_s = 0.21$, | | |
| clustering coefficient | (0.25) | 0.04* | p = 0.76 | p = 0.12 | | |
| Small-world | 3.57 | $r_s = 0.23, p =$ | $r_s = -0.04$, | $r_s = 0.17$, | | |
| coefficient | (0.18) | 0.077 | p = 0.77 | p = 0.2 | | |
| Local ^c | | | | | | |
| Gray matter connec | tomes ^d | | | | | |
| Path length | | | | | | |
| Right | | $r_s = -0.33$, | | | | |
| temporal pole | | p = 0.01, | | | | |
| | | $p_{FDR}=0.20$ | | | | |
| Normalized path length | | | | | | |
| Right | | $r_s = -0.38, p =$ | | | | |
| temporal pole | | $0.004, p_{FDR} = 0.069$ | | | | |
| DTI connectomes | | | | | | |
| Normalized path le | ength | | | | | |
| Left superior | - | $r_s = 0.27$, | | | | |
| medial frontal | | p = 0.0447, | | | | |
| gyrus | | $p_{FDR} = 0.76$ | | | | |
| Normalized cluster | ring coeffici | ent | | | | |
| Left angular | | $r_s = 0.43, p <$ | | | | |
| gyrus | | $0.001, p_{FDR} = 0.01*$ | | | | |
| Small-world coeffi | cient | | | | | |
| Left angular | | $r_s = 0.37, p =$ | | | | |
| gyrus | | $0.0039, p_{FDR} = 0.07$ | | | | |

Abbreviations: BCIS=Beck Cognitive Insight Scale; SR = self-reflectiveness subscale; SC = self-certainty subscale; CI = composite index score.

2015, 2014; van der Meer et al., 2013), and even more consistently in poorer *clinical* insight (i.e. illness awareness) in patients with schizophrenia and individuals at ultra-high risk (e.g. Clark et al., 2018; Gerretsen et al., 2014; Liemburg et al., 2012). Clark et al., for example, found that a strongly connected DMN was associated with poor insight into subthreshold psychotic symptoms in ultra-high risk adolescents and young adults (Clark et al., 2018). Most of these studies found that lower self-reflectiveness or clinical insight was associated with lower activation in or connectivity of DMN-regions (Buchy et al., 2015, 2014; Liemburg et al., 2012; van der Meer et al., 2013). Our study supplements results of

previous studies by showing that temporal dynamics of functional networks are also related to cognitive insight. The strength of activation or connectivity within functional networks or the whole brain was not examined in this study. Indeed, the positive relationship between self-reflectiveness or clinical insight and brain activation of DMN-regions does not preclude our finding of a negative relationship between self-reflectiveness and lifetime of the DMN-state.

Results of our study showed that, in individuals with lower selfreflectiveness, the probabilities of switching to the DMN-state were higher from a state involving regions of the ventral attention network (Yeo et al., 2011). The ventral attention network likely reflects a combination of the salience (Seeley et al., 2007) and cingulo-opercular networks (Dosenbach et al., 2007; Yeo et al., 2011). The insula plays an important role within the salience network, mediating the switch between interoceptive DMN function and exteroceptive task-externally oriented attention (Menon and Uddin, 2010). It has been implicated in interoceptive awareness as well as higher-order cognitive processes such as cognitive control and attention (Menon and Uddin, 2010). Insular abnormalities were found to be related to poorer (meta)cognitive insight in patients with a psychotic disorder in earlier studies (Caletti et al., 2017; Spalletta et al., 2014). One could argue that dwelling longer in the ventral attention network and switching less back to the DMN could enhance "being in touch with oneself" in a quite literal way as this network is involved in the representation of awareness of bodily states (Damasio, 1999). It should be noted that no correction for multiple testing was applied, however, so no strong conclusions can be drawn from this result without replication in future studies. Tentatively, our results could suggest that people with lower levels of insight may have less access to their own emotional states.

Altogether, our FC findings imply less stable functional networks (implicated by increased switching frequency), less global integration (implicated by lower time spent in the globally synchronized state) and an overly present DMN in individuals with poorer cognitive insight, and poorer self-reflectiveness specifically. An explanation for our results that individuals with lower cognitive insight spend less time in the globally synchronized baseline state, could be that in these individuals the transition towards specialized networks is more difficult, rendering more frequent switching between states, less stable functional networks and an overly present DMN.

4.2. Structural connectivity

Reoccurring patterns of FC might reinforce structural connections. Since our FC findings imply less stable functional networks and less global integration, one would expect reduced segregation and integration of structural connectomes. For self-reflectiveness, our results for the DTI connectomes indeed suggest less stable or segregated structural networks, as implicated by significantly lower clustering coefficient. However, we did not find reduced integration (reflected by path length) in the DTI connectome. When examining the relationship between brain function and structure further, we found that less anatomical segregation into clearly-defined networks (i.e. lower clustering coefficient) was related to less stable functional networks (i.e. higher switching frequency) and spending more time in the DMN (i.e. higher probability of the DMN-state).

Given our finding of a relationship between self-reflectiveness and temporal dynamics of the DMN, one would expect structural abnormalities of DMN-regions in addition to global structural abnormalities. With regard to the DTI connectome, we indeed found that individuals with lower self-reflectiveness show decreased segregation (i.e. lower clustering coefficient and trend-level lower small-world coefficients), indicating lower embeddedness, of the left angular gyrus with the rest of the brain. When linking function to structure, reduced small-world coefficients of the left angular gyrus were related to longer time spent in and higher probability of occurrence of the DMN-State. This is in line with fMRI- and PET-studies that identified the angular gyrus as a key

^a Corrected for total gray matter volume.

^b Not trend-level significant anymore after additional correction for density (which was correlated with BCIS CI).

 $^{^{\}rm c}$ Locally, only correlations between self-reflectiveness and local graph metrics of regions of State 3 were calculated. Correlations significant at p_{uncorrected}<0.05 are reported. FDR-correction for 17 tests (i.e. 17 regions in State 3).

^d Corrected for total and local gray matter volume.

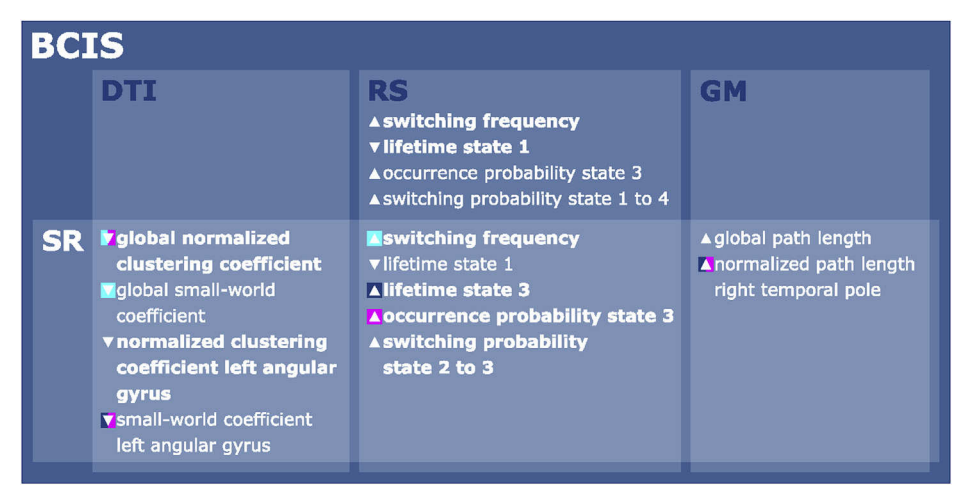


Fig. 6. Overview of all results.

Correlations between BCIS composite index scores (top row 'BCIS') and BCIS self-reflectiveness (bottom row 'SR') on one hand and characteristics of DTI-connectomes (column 'DTI'), time-varying dynamics of resting-state functional connectivity (column 'RS') and gray matter connectomes (column 'GM') on the other hand. No significant correlations were found with BCIS self-certainty (SC). Significant correlations are displayed in bold text; trend-level significance in regular text. Triangles indicate the direction of the correlation with lower cognitive insight (i.e. lower BCIS composite index score, lower SR, higher SC; e.g. lower BCIS is associated with higher switching frequency). In color, significant correlations between resting-state functional connectivity characteristics and structural characteristics (e.g., lifetime State 3 is related to small-world coefficient left angular gyrus of DTIconnectome and normalized path length of right temporal pole GM-connectome).

Abbreviations: BCIS=Beck Cognitive Insight Scale composite index score; SR = self-reflectiveness subscale of BCIS; SC = self-certainty subscale of BCIS; DTI = diffusion tensor imaging; RS = resting-state fMRI; GM = gray matter.

region of the DMN (Greicius et al., 2003; Raichle et al., 2001; Uddin et al., 2009). The angular gyrus has not been linked to *cognitive* insight in previous studies, although one study found that increased connectivity in the DMN with the left angular gyrus was associated with poorer *clinical* insight in schizophrenia (Gerretsen et al., 2014).

No studies on the relationship between cognitive insight and structural connectivity have been conducted in healthy individuals before. Two earlier DTI-studies did not find significant correlations with cognitive insight nor its subdimensions in schizophrenia (Ćurčić-Blake et al., 2015; Orfei et al., 2013). This is the first study examining the DTI-connectome, however. Altogether, our results suggest that individuals with lower self-reflectiveness show lower structural embeddedness of the angular gyrus, a key region of the DMN, and that this is associated with an overly present DMN.

With regard to gray matter network structure, we only found associations with self-reflectiveness at trend-level significance. Our results show that lower self-reflectiveness was related to lower global (implicated by higher path length) integration as well as local integration of the right temporal pole. When linking structure to function, higher path length of the right temporal pole was associated with a higher time spent in and probability of occurrence of the DMN-state. No firm conclusions can be drawn without replication of our results in other samples, given that we only found associations at trend-level significance.

4.3. Strengths and limitations

The LEiDA-method allowed us to investigate time-varying dynamics of resting state FC while taking FC per timepoint into account. Advantages of this method are that 1) temporally delayed relationships can be captured with phase coherence techniques (Lord et al., 2019), 2) no window size has to be chosen in contrast to the sliding window approach and, 3) there is less influence of high-frequency noise. The combination of MRI-data of different modalities allowed us to get a more comprehensive view of the neural substrate of cognitive insight. This study has several limitations. First, as the first study investigating dynamic connectivity correlates of cognitive insight, our study had an exploratory nature and needs replication in an independent sample. Second, to limit false negatives and to enhance the probability of hypothesis-generating findings at this early stage of investigation into the dynamic correlates of insight, we did not apply the strictest method to correct for multiple testing. This comes at the cost of an increased risk for false positives.

Third, the relatively coarse AAL-parcellation was used for all modalities, in order to replicate methods of earlier studies to aid interpretation and comparison of our results. For fMRI-data, a more fine-grained parcellation based on FC (instead of structure) might yield further breakdown into smaller subnetworks (Craddock et al., 2012; Gordon et al., 2016; Hallquist and Hillary, 2019). Future studies could examine the effect of different parcellations on functional connectivity states and how time-varying dynamics of these states relate to cognitive insight. Fourth, most tractography techniques underestimate long-range connections, and probabilistic tractography might lead to false positives which have shown to have a bigger influence on graph metrics than false negatives (Zalesky et al., 2016). However, this is only expected to diminish the association between DTI graph metrics and cognitive insight. With regard to the gray matter connectome, density differed between individuals as connectomes were binarized by applying a subject-specific threshold. Density is highly correlated with higher-order graph metrics such as path length and clustering coefficient. Keeping densities similar across individuals might yield false-positive connections, however, therefore, we chose to exactly replicate the existing method of Tijms et al. (2012).

4.4. Conclusions

Our results show converging evidence that functional and structural networks of individuals with lower cognitive insight, and more specifically poorer self-reflectiveness, are less stable. An overly present DMN appears to play a key role. It is unclear, however, whether this generalizes to neurological or psychiatric disorders characterized by poor insight, such as schizophrenia. If replicated, our findings could have practical implications, e.g. inform interventions that reinforce functional networks (e.g. neurofeedback) or decrease mind-wandering (e.g. mindfulness mediation training) (Mooneyham et al., 2016; Mrazek et al., 2013; Zanesco et al., 2016). First and foremost, our results provide information on the basic neural underpinnings of insight into mental processes and support the use of dynamic connectivity analysis and multimodal imaging to gain a further understanding of mental processes that are so central to the human condition.

Funding

This work was supported by the University Medical Center Groningen, The Netherlands. JC is supported by the Portuguese Foundation for

Science and Technology (grant number CEECIND/03325/2017). The funding sources had no role in study design, data collection and analysis, decision to publish, or preparation of the manuscript.

Declarations of competing interest

None.

CRediT authorship contribution statement

Daouia I. Larabi: Conceptualization, Methodology, Software, Formal analysis, Visualization, Writing - original draft, Writing - review & editing, Project administration. Remco J. Renken: Methodology, Software, Resources, Validation, Writing - review & editing. Joana Cabral: Methodology, Software, Resources, Visualization, Writing - review & editing. Jan-Bernard C. Marsman: Methodology, Software, Resources, Validation, Writing - review & editing. André Aleman: Conceptualization, Resources, Supervision, Writing - review & editing, Funding acquisition. Branislava Ćurčić-Blake: Conceptualization, Methodology, Software, Formal analysis, Validation, Supervision, Writing - review & editing.

Acknowledgements

The authors would like to thank all participants for their participation, Anita Sibeijn-Kuiper and Judith Streurman for support in scanning participants, Dr. Michelle Servaas and Dr. Leonardo Cerliani for advice on analyses, and the Center for Magnetic Resonance Research of the University of Minnesota for receipt of their multi-echo-EPI sequence. We would also like to thank the Center for Information Technology of the University of Groningen for their support and for providing access to the Peregrine high-performance computing cluster.

Appendix A. Supplementary data

Supplementary data to this article can be found online at https://doi.org/10.1016/j.neuroimage.2020.116896.

References

- Alexander-Bloch, A., Raznahan, A., Bullmore, E., Giedd, J., 2013. The convergence of maturational change and structural covariance in human cortical networks. J. Neurosci. 33, 2889–2899. https://doi.org/10.1523/JNEUROSCI.3554-12.2013.
- Andersson, J.L.R., Sotiropoulos, S.N., 2016. An integrated approach to correction for off-resonance effects and subject movement in diffusion MR imaging. Neuroimage 125, 1063–1078. https://doi.org/10.1016/j.neuroimage.2015.10.019.
- Andrews-Hanna, J.R., Smallwood, J., Spreng, R.N., 2014. The default network and self-generated thought: component processes, dynamic control, and clinical relevance. Ann. N. Y. Acad. Sci. 1316, 29–52. https://doi.org/10.1111/nyas.12360.
- Andrews-Hanna, J.R., Snyder, A.Z., Vincent, J.L., Lustig, C., Head, D., Raichle, M.E.E., Buckner, R.L., 2007. Disruption of large-scale brain systems in advanced aging. Neuron 56, 924–935. https://doi.org/10.1016/j.neuron.2007.10.038.
- Beck, A.T., Baruch, E., Balter, J.M., Steer, R.A., Warman, D.M., 2004. A new instrument for measuring insight: the Beck Cognitive Insight Scale. Schizophr. Res. 68, 319–329. https://doi.org/10.1016/S0920-9964(03)00189-0.
- Beckmann, C.F., DeLuca, M., Devlin, J.T., Smith, S.M., 2005. Investigations into restingstate connectivity using independent component analysis. Philos. Trans. R. Soc. B Biol. Sci. 360, 1001–1013. https://doi.org/10.1098/rstb.2005.1634.
- Behrens, T.E.J., Berg, H.J., Jbabdi, S., Rushworth, M.F.S., Woolrich, M.W., 2007. Probabilistic diffusion tractography with multiple fibre orientations: what can we gain? Neuroimage 34, 144–155. https://doi.org/10.1016/ineuroimage.2006.09.018.
- Behrens, T.E.J., Woolrich, M.W., Jenkinson, M., Johansen-Berg, H., Nunes, R.G., Clare, S., Matthews, P.M., Brady, J.M., Smith, S.M., 2003. Characterization and propagation of uncertainty in diffusion-weighted MR imaging. Magn. Reson. Med. 50, 1077–1088. https://doi.org/10.1002/mrm.10609.
- Bijsterbosch, J.D., Woolrich, M.W., Glasser, M.F., Robinson, E.C., Beckmann, C.F., Van Essen, D.C., Harrison, S.J., Smith, S.M., 2018. The relationship between spatial configuration and functional connectivity of brain regions. Elife 7, e32992. https:// doi.org/10.7554/eLife.32992.
- Biswal, B., Zerrin Yetkin, F., Haughton, V.M., Hyde, J.S., 1995. Functional connectivity in the motor cortex of resting human brain using echo-planar mri. Magn. Reson. Med. 34, 537–541. https://doi.org/10.1002/mrm.1910340409.

- Buchy, L., Hawco, C., Bodnar, M., Izadi, S., Dell'Elce, J., Messina, K., Lepage, M., 2014. Functional magnetic resonance imaging study of external source memory and its relation to cognitive insight in non-clinical subjects. Psychiatr. Clin. Neurosci. 68, 683–691. https://doi.org/10.1111/pcn.12177.
- Buchy, L., Hawco, C., Joober, R., Malla, A., Lepage, M., 2015. Cognitive insight in first-episode schizophrenia: further evidence for a role of the ventrolateral prefrontal cortex. Schizophr. Res. 166, 65–68. https://doi.org/10.1016/j.schres.2015.05.009.
- Cabral, J., Vidaurre, D., Marques, P., Magalhães, R., Silva Moreira, P., Miguel Soares, J., Deco, G., Sousa, N., Kringelbach, M.L., 2017. Cognitive performance in healthy older adults relates to spontaneous switching between states of functional connectivity during rest. Sci. Rep. 7 https://doi.org/10.1038/s41598-017-05425-7.
- Caletti, E., Marotta, G., Del Vecchio, G., Paoli, R.A., Gigliobianco, M., Prunas, C., Zugno, E., Bottinelli, F., Brambilla, P., Altamura, A.C., 2017. The metabolic basis of cognitive insight in psychosis: a positron emission tomography study. PloS One 12, e0175803. https://doi.org/10.1371/journal.pone.0175803.
- Christoff, K., Gordon, A.M., Smallwood, J., Smith, R., Schooler, J.W., 2009. Experience sampling during fMRI reveals default network and executive system contributions to mind wandering. Proc. Natl. Acad. Sci. Unit. States Am. 106, 8719–8724. https:// doi.org/10.1073/pnas.0900234106.
- Clark, S.V., Mittal, V.A., Bernard, J.A., Ahmadi, A., King, T.Z., Turner, J.A., 2018. Stronger default mode network connectivity is associated with poorer clinical insight in youth at ultra high-risk for psychotic disorders. Schizophr. Res. 193, 244–250. https://doi.org/10.1016/j.schres.2017.06.043.
- Cox, R.W., 1996. AFNI: Software for analysis and visualization of functional magnetic resonance neuroimages. Comput. Biomed. Res. 29, 162–173. https://doi.org/ 10.1006/cbmr.1996.0014.
- Craddock, R.C., James, G.A., Holtzheimer, P.E., Hu, X.P., Mayberg, H.S., 2012. A whole brain fMRI atlas generated via spatially constrained spectral clustering. Hum. Brain Mapp. 33, 1914–1928. https://doi.org/10.1002/hbm.21333.
- Cui, G., Wang, Y., Wang, X., Zheng, L., Li, L., Li, P., Zhang, L., Guo, Y., Chen, Y., Sun, Z., Meng, X., 2020. Static and dynamic functional connectivity of the prefrontal cortex during resting-state predicts self-serving bias in depression. Behav. Brain Res. 379, 112335. https://doi.org/10.1016/j.bbr.2019.112335.
- Ćurčić-Blake, B., van der Meer, L., Pijnenborg, G.H.M., David, A.S., Aleman, A., 2015. Insight and psychosis: functional and anatomical brain connectivity and self-reflection in Schizophrenia. Hum. Brain Mapp. 36, 4859–4868. https://doi.org/10.1002/hbm.22955.
- Dam, J., 2006. Insight in schizophrenia: a review. Nord. J. Psychiatry 60, 114–120. https://doi.org/10.1080/08039480600600185.
- Damasio, A.R., 1999. The Feeling of what Happens: Body, Emotion and the Making of Consciousness. Harcourt Trade Publishers. New York.
- Damoiseaux, J.S., Rombouts, S.A.R.B., Barkhof, F., Scheltens, P., Stam, C.J., Smith, S.M., Beckmann, C.F., 2006. Consistent resting-state networks across healthy subjects. Proc. Natl. Acad. Sci. Unit. States Am. 103, 13848–13853. https://doi.org/10.1073/pnas.0601417103.
- De Luca, M., Beckmann, C.F., De Stefano, N., Matthews, P.M., Smith, S.M., 2006. fMRI resting state networks define distinct modes of long-distance interactions in the human brain. Neuroimage 29, 1359–1367. https://doi.org/10.1016/ineuroimage.2005.08.035.
- Donahue, C.J., Sotiropoulos, S.N., Jbabdi, S., Hernandez-Fernandez, M., Behrens, T.E., Dyrby, T.B., Coalson, T., Kennedy, H., Knoblauch, K., Van Essen, D.C., Glasser, M.F., 2016. Using diffusion tractography to predict cortical connection strength and distance: a quantitative comparison with tracers in the monkey. J. Neurosci. 36, 6758–6770. https://doi.org/10.1523/jneurosci.0493-16.2016.
- Dosenbach, N.U.F., Fair, D.A., Miezin, F.M., Cohen, A.L., Wenger, K.K., Dosenbach, R.A.T., Fox, M.D., Snyder, A.Z., Vincent, J.L., Raichle, M.E., Schlaggar, B.L., Petersen, S.E., 2007. Distinct brain networks for adaptive and stable task control in humans. Proc. Natl. Acad. Sci. Unit. States Am. 104, 11073–11078. https://doi.org/10.1073/pnas.0704320104.
- Dunn, J.C., 1973. A fuzzy relative of the ISODATA process and its use in detecting compact well-separated clusters. J. Cybern. 3, 32–57. https://doi.org/10.1080/ 01969727308546046.
- Essen, D.C. Van, 1997. A tension-based theory of morphogenesis and compact wiring in the central nervous system. Nature 385, 313–318. https://doi.org/10.1038/ 38531330
- Evans, A.C., 2013. Networks of anatomical covariance. Neuroimage 80, 489–504. https://doi.org/10.1016/j.neuroimage.2013.05.054.
- Feinberg, D.A., Moeller, S., Smith, S.M., Auerbach, E., Ramanna, S., Glasser, M.F., Miller, K.L., Ugurbil, K., Yacoub, E., 2010. Multiplexed echo planar imaging for subsecond whole brain fmri and fast diffusion imaging. PloS One 5, e15710. https:// doi.org/10.1371/journal.pone.0015710.
- Figueroa, C.A., Cabral, J., Mocking, R.J.T., Rapuano, K.M., van Hartevelt, T.J., Deco, G., Expert, P., Schene, A.H., Kringelbach, M.L., Ruhé, H.G., 2019. Altered ability to access a clinically relevant control network in patients remitted from major depressive disorder. Hum. Brain Mapp. 40, 2771–2786. https://doi.org/10.1002/hbm.24559.
- Fong, A.H.C., Yoo, K., Rosenberg, M.D., Zhang, S., Li, C.-S.R., Scheinost, D., Constable, R.T., Chun, M.M., 2019. Dynamic functional connectivity during task performance and rest predicts individual differences in attention across studies. Neuroimage 188, 14–25. https://doi.org/10.1016/j.neuroimage.2018.11.057.
- Fornito, A., Bullmore, E.T., 2015. Reconciling abnormalities of brain network structure and function in schizophrenia. Curr. Opin. Neurobiol. https://doi.org/10.1016/ j.conb.2014.08.006.
- Gerretsen, P., Menon, M., Mamo, D.C., Fervaha, G., Remington, G., Pollock, B.G., Graff-Guerrero, A., 2014. Impaired insight into illness and cognitive insight in

- schizophrenia spectrum disorders: resting state functional connectivity. Schizophr. Res. 160, 43–50. https://doi.org/10.1016/j.schres.2014.10.015.
- Glerean, E., Salmi, J., Lahnakoski, J.M., Jääskeläinen, I.P., Sams, M., 2012. Functional magnetic resonance imaging phase synchronization as a measure of dynamic functional connectivity. Brain Connect. 2, 91–101. https://doi.org/10.1089/ brain.2011.0068.
- Goldstein, R.Z., Craig, A.D., Bechara, A., Garavan, H., Childress, A.R., Paulus, M.P., Volkow, N.D., 2009. The neurocircuitry of impaired insight in drug addiction. Trends Cognit. Sci. 13, 372–380. https://doi.org/10.1016/j.tics.2009.06.004.
- Gong, G., He, Y., Chen, Z.J., Evans, A.C., 2012. Convergence and divergence of thickness correlations with diffusion connections across the human cerebral cortex. Neuroimage 59, 1239–1248. https://doi.org/10.1016/j.neuroimage.2011.08.017.
- Gordon, E.M., Laumann, T.O., Adeyemo, B., Huckins, J.F., Kelley, W.M., Petersen, S.E., 2016. Generation and evaluation of a cortical area parcellation from resting-state correlations. Cerebr. Cortex 26, 288–303. https://doi.org/10.1093/cercor/bhu239.
- Greicius, M.D., Krasnow, B., Reiss, A.L., Menon, V., 2003. Functional connectivity in the resting brain: a network analysis of the default mode hypothesis. Proc. Natl. Acad. Sci. Unit. States Am. 100, 253–258. https://doi.org/10.1073/pnas.0135058100.
- Hallquist, M.N., Hillary, F.G., 2019. Graph theory approaches to functional network organization in brain disorders: a critique for a brave new small-world. Netw. Neurosci. 3, 1–26. https://doi.org/10.1162/netn_a_00054.
- Hilgetag, C.C., Barbas, H., 2005. Developmental mechanics of the primate cerebral cortex. Anat. Embryol. 210, 411–417. https://doi.org/10.1007/s00429-005-0041-5.
- Jenkinson, M., Bannister, P., Brady, M., Smith, S., 2002. Improved optimization for the robust and accurate linear registration and motion correction of brain images. Neuroimage 17, 825–841. https://doi.org/10.1016/S1053-8119(02)91132-8.
- Jenkinson, M., Smith, S., 2001. A global optimisation method for robust affine registration of brain images. Med. Image Anal. 5, 143–156. https://doi.org/10.1016/ S1361-8415(01)00036-6.
- Keller, C.J., Bickel, S., Honey, C.J., Groppe, D.M., Entz, L., Craddock, R.C., Lado, F.A., Kelly, C., Milham, M., Mehta, A.D., 2013. Neurophysiological investigation of spontaneous correlated and anticorrelated fluctuations of the BOLD signal. J. Neurosci. 33, 6333–6342. https://doi.org/10.1523/jneurosci.4837-12.2013.
- Kimhy, D., Jobson-Ahmed, L., Ben-David, S., Ramadhar, L., Malaspina, D., Corcoran, C.M., 2014. Cognitive insight in individuals at clinical high risk for psychosis. Early Interv. Psychiatry 8, 130–137. https://doi.org/10.1111/eip.12023.
- Kucyi, A., Hove, M.J., Esterman, M., Hutchison, R.M., Valera, E.M., 2017. Dynamic brain network correlates of spontaneous fluctuations in attention. Cerebr. Cortex 27, 1831–1840. https://doi.org/10.1093/cercor/bhw029.
- Kucyi, A., Tambini, A., Sadaghiani, S., Keilholz, S., Cohen, J.R., 2018. Spontaneous cognitive processes and the behavioral validation of time-varying brain connectivity. Netw. Neurosci. 2, 397–417. https://doi.org/10.1162/netn_a_00037.
- Kundu, P., Brenowitz, N.D., Voon, V., Worbe, Y., Vertes, P.E., Inati, S.J., Saad, Z.S., Bandettini, P.A., Bullmore, E.T., 2013. Integrated strategy for improving functional connectivity mapping using multiecho fMRI. Proc. Natl. Acad. Sci. Unit. States Am. 110, 16187–16192. https://doi.org/10.1073/pnas.1301725110.
- Kundu, P., Inati, S.J., Evans, J.W., Luh, W.M., Bandettini, P.A., 2012. Differentiating BOLD and non-BOLD signals in fMRI time series using multi-echo EPI. Neuroimage 60, 1759–1770. https://doi.org/10.1016/j.jpeuroimage.2011.12.028
- 60, 1759–1770. https://doi.org/10.1016/j.neuroimage.2011.12.028.
 Lee, J.S., Chun, J.W., Lee, S.H., Kim, E., Lee, S.K., Kim, J.J., 2015. Altered neural basis of the reality processing and its relation to cognitive insight in schizophrenia. PloS One 10, 1–15. https://doi.org/10.1371/journal.pone.0120478.
- Liemburg, E.J., van der Meer, L., Swart, M., Curcic-Blake, B., Bruggeman, R., Knegtering, H., Aleman, A., 2012. Reduced connectivity in the self-processing network of schizophrenia patients with poor insight. PloS One 7, 1–9. https:// doi.org/10.1371/journal.pone.0042707.
- Lincoln, T.M., Lullmann, E., Rief, W., 2007. Correlates and long-term consequences of poor insight in patients with schizophrenia. A systematic review. Schizophr. Bull. 33, 1324–1342. https://doi.org/10.1093/schbul/sbm002.
- Llera, A., Wolfers, T., Mulders, P., Beckmann, C.F., 2019. Inter-individual differences in human brain structure and morphology link to variation in demographics and behavior. Elife. https://doi.org/10.7554/eLife.44443 e44443.
- Lord, L.-D., Expert, P., Atasoy, S., Roseman, L., Rapuano, K., Lambiotte, R., Nutt, D.J., Deco, G., Carhart-Harris, R.L., Kringelbach, M.L., Cabral, J., 2019. Dynamical exploration of the repertoire of brain networks at rest is modulated by psilocybin. Neuroimage 199, 127–142. https://doi.org/10.1016/j.neuroimage.2019.05.060.
- Mangone, C.A., Hier, D.B., Gorelick, P.B., Ganellen, R.J., Langenberg, P., Boarman, R., Dollear, W.C., 1991. Impaired insight in alzheimer's disease. J. Geriatr. Psychiatr. Neurol. 4, 189–193. https://doi.org/10.1177/089198879100400402.
- Mason, M.F., Norton, M.I., Van Horn, J.D., Wegner, D.M., Grafton, S.T., Macrae, C.N., 2007. Wandering minds: the default network and stimulus-independent thought. Science 84 315, 393–395. https://doi.org/10.1126/science.1131295.
- Matsunaga, H., Kiriike, N., Matsui, T., Oya, K., Iwasaki, Y., Koshimune, K., Miyata, A., Stein, D.J., 2002. Obsessive-compulsive disorder with poor insight. Compr. Psychiatr. 43, 150–157. https://doi.org/10.1053/comp.2002.30798.
- Menon, V., Uddin, L.Q., 2010. Saliency, switching, attention and control: a network model of insula function. Brain Struct. Funct. https://doi.org/10.1007/s00429-010-0262-0.
- Moeller, S., Yacoub, E., Olman, C.A., Auerbach, E., Strupp, J., Harel, N., Uğurbil, K., 2010.
 Multiband multislice GE-EPI at 7 tesla, with 16-fold acceleration using partial parallel imaging with application to high spatial and temporal whole-brain fMRI. Magn.
 Reson. Med. 63, 1144–1153. https://doi.org/10.1002/mrm.22361.
- Mooneyham, B.W., Mrazek, M.D., Mrazek, A.J., Schooler, J.W., 2016. Signal or noise: brain network interactions underlying the experience and training of mindfulness. Ann. N. Y. Acad. Sci. 1369, 240–256. https://doi.org/10.1111/nyas.13044.

- Mrazek, M.D., Franklin, M.S., Phillips, D.T., Baird, B., Schooler, J.W., 2013. Mindfulness training improves working memory capacity and GRE performance while reducing mind wandering. Psychol. Sci. 24, 776–781. https://doi.org/10.1177/ 0056707613450659
- Murphy, K., Fox, M.D., 2017. Towards a consensus regarding global signal regression for resting state functional connectivity MRI. Neuroimage 154, 169–173. https:// doi.org/10.1016/j.neuroimage.2016.11.052.
- Nair, A., Palmer, E.C., Aleman, A., David, A.S., 2014. Relationship between cognition, clinical and cognitive insight in psychotic disorders: a review and meta-analysis. Schizophr. Res. 152, 191–200. https://doi.org/10.1016/j.schres.2013.11.033.
- Nomi, J.S., Vij, S.G., Dajani, D.R., Steimke, R., Damaraju, E., Rachakonda, S., Calhoun, V.D., Uddin, L.Q., 2017. Chronnectomic patterns and neural flexibility underlie executive function. Neuroimage 147, 861–871. https://doi.org/10.1016/ j.neuroimage.2016.10.026.
- Northoff, G., Heinzel, A., de Greck, M., Bermpohl, F., Dobrowolny, H., Panksepp, J., 2006. Self-referential processing in our brain-A meta-analysis of imaging studies on the self. Neuroimage 31, 440–457. https://doi.org/10.1016/j.neuroimage.2005.12.002.
- Oldfield, R.C., 1971. The assessment and analysis of handedness: the Edinburgh inventory. Neuropsychologia 9, 97–113. https://doi.org/10.1016/0028-3932(71)
- Orfei, M.D., Piras, F., Macci, E., Caltagirone, C., Spalletta, G., 2013. The neuroanatomical correlates of cognitive insight in schizophrenia. Soc. Cognit. Affect Neurosci. 8, 418–423. https://doi.org/10.1093/scan/nss016.
- Posse, S., Wiese, S., Gembris, D., Mathiak, K., Kessler, C., Grosse-Ruyken, M.L., Elghahwagi, B., Richards, T., Dager, S.R., Kiselev, V.G., 1999. Enhancement of BOLDcontrast sensitivity by single-shot multi-echo functional MR imaging. Magn. Reson. Med. 42, 87–97. https://doi.org/10.1002/(SICI)1522-2594(199907)42:1<87 ::AID-MRM13>3.0.CO;2-O.
- Power, J.D., Barnes, K.A., Snyder, A.Z., Schlaggar, B.L., Petersen, S.E., 2012. Spurious but systematic correlations in functional connectivity MRI networks arise from subject motion. Neuroimage 59, 2142–2154. https://doi.org/10.1016/ j.neuroimage.2011.10.018.
- Qin, P., Northoff, G., 2011. How is our self related to midline regions and the default-mode network? Neuroimage. https://doi.org/10.1016/j.neuroimage.2011.05.028.
- R Core team, 2018. R Core Team. R A lang. Environ. Stat. Comput. R Found. Stat. Comput., Vienna, Austria. URL. http://www.R-project.org/.
- Raichle, M.E., MacLeod, A.M., Snyder, A.Z., Powers, W.J., Gusnard, D.A., Shulman, G.L., 2001. A default mode of brain function. Proc. Natl. Acad. Sci. Unit. States Am. 98, 676–682. https://doi.org/10.1073/pnas.98.2.676.
- Raine, A., 1991. The SPQ: a scale for the assessment of schizotypal personality based on DSM-III-R criteria. Schizophr. Bull. 17, 555–564. https://doi.org/10.1093/schbul/
- Riggs, S.E., Grant, P.M., Perivoliotis, D., Beck, A.T., 2012. Assessment of cognitive insight: a qualitative review. Schizophr. Bull. 38, 338–350. https://doi.org/10.1093/schbul/ sbq085.
- Rubinov, M., Sporns, O., 2010. Complex network measures of brain connectivity: uses and interpretations. Neuroimage 52, 1059–1069. https://doi.org/10.1016/ j.neuroimage.2009.10.003.
- Schmitt, J.E., Lenroot, R.K., Ordaz, S.E., Wallace, G.L., Lerch, J.P., Evans, A.C., Prom, E.C., Kendler, K.S., Neale, M.C., Giedd, J.N., 2009. Variance decomposition of MRI-based covariance maps using genetically informative samples and structural equation modeling. Neuroimage 47, 56–64. https://doi.org/10.1016/j.neuroimage.2008.06.039.
- Scholvinck, M.L., Maier, A., Ye, F.Q., Duyn, J.H., Leopold, D.A., 2010. Neural basis of global resting-state fMRI activity. Proc. Natl. Acad. Sci. Unit. States Am. 107, 10238–10243. https://doi.org/10.1073/pnas.0913110107.
- Seeley, W.W., Crawford, R.K., Zhou, J., Miller, B.L., Greicius, M.D., 2009. Neurodegenerative diseases target large-scale human brain networks. Neuron 62, 42–52. https://doi.org/10.1016/j.neuron.2009.03.024.
- Seeley, W.W., Menon, V., Schatzberg, A.F., Keller, J., Glover, G.H., Kenna, H., Reiss, A.L., Greicius, M.D., 2007. Dissociable intrinsic connectivity networks for salience processing and executive control. J. Neurosci. 27, 2349–2356. https://doi.org/ 10.1523/jneurosci.5587-06.2007.
- Smallwood, J., Schooler, J.W., 2015. The science of mind wandering: empirically navigating the stream of consciousness. Annu. Rev. Psychol. 66, 487–518. https:// doi.org/10.1146/annurev-psych-010814-015331.
- Smith, S.M., 2002. Fast robust automated brain extraction. Hum. Brain Mapp. 17, 143–155. https://doi.org/10.1002/hbm.10062.
- Spalletta, G., Piras, F.F., Piras, F.F., Caltagirone, C., Orfei, M.M.D., 2014. The structural neuroanatomy of metacognitive insight in schizophrenia and its psychopathological and neuropsychological correlates. Hum. Brain Mapp. 35, 4729–4740. https:// doi.org/10.1002/hbm.22507.
- Sporns, O., Chialvo, D.R., Kaiser, M., Hilgetag, C.C., 2004. Organization, development and function of complex brain networks. Trends Cognit. Sci. https://doi.org/ 10.1016/j.tics.2004.07.008.
- Stark, E., Cabral, J., Riem, M.M.E., van Ijzendoorn, M.H., Stein, A., Kringelbach, M.L., 2019. The power of smiling: the adult brain networks underlying learned infant temperament. Cerebr. Cortex.
- Startup, M., 1997. Awareness of own and others' schizophrenic illness. Schizophr. Res. 26, 203–211. https://doi.org/10.1016/S0920-9964(97)00050-9.
- Sun, F., Zhao, Z., Lan, M., Xu, Y., Huang, M., Xu, D., 2020. Abnormal dynamic functional network connectivity of the mirror neuron system network and the mentalizing network in patients with adolescent-onset, first-episode, drug-naïve schizophrenia. Neurosci. Res. https://doi.org/10.1016/j.jhazmat.2019.121407 (in press).

- Tijms, B.M., Seris, P., Willshaw, D.J., Lawrie, S.M., 2012. Similarity-based extraction of individual networks from gray matter MRI scans. Cerebr. Cortex 22, 1530–1541. https://doi.org/10.1093/cercor/bhr221.
- Tzourio-Mazoyer, N., Landeau, B., Papathanassiou, D., Crivello, F., Etard, O., Delcroix, N., Mazoyer, B., Joliot, M., 2002. Automated anatomical labeling of activations in SPM using a macroscopic anatomical parcellation of the MNI MRI single-subject brain. Neuroimage 15, 273–289. https://doi.org/10.1006/nimg.2001.0978.
- Uchida, T., Matsumoto, K., Ito, F., Ohmuro, N., Miyakoshi, T., Ueno, T., Matsuoka, H., 2014. Relationship between cognitive insight and attenuated delusional symptoms in individuals with at-risk mental state. Psychiatr. Res. 217, 20–24. https://doi.org/ 10.1016/j.psychres.2014.01.003.
- Uddin, L.Q., Kelly, A.M.C., Biswal, B.B., Castellanos, F.X., Milham, M.P., 2009. Functional connectivity of default mode network components: correlation, anticorrelation, and causality. Hum. Brain Mapp. 30, 625–637. https://doi.org/10.1002/hbm.20531.
- van der Meer, L., Costafreda, S., Aleman, A., David, A.S., 2010. Self-reflection and the brain: a theoretical review and meta-analysis of neuroimaging studies with implications for schizophrenia. Neurosci. Biobehav. Rev. 34, 935–946. https:// doi.org/10.1016/j.neubiorev.2009.12.004.
- van der Meer, L., de Vos, A.E., Stiekema, A.P.M., Pijnenborg, G.H.M., Van Tol, M.J., Nolen, W.A., David, A.S., Aleman, A., 2013. Insight in schizophrenia: involvement of self-reflection networks? Schizophr. Bull. (Arch. Am. Art) 39, 1288–1295. https:// doi.org/10.1093/schbul/sbs122.
- van Wijk, B.C.M., Stam, C.J., Daffertshofer, A., 2010. Comparing brain networks of different size and connectivity density using graph theory. PloS One 5. https:// doi.org/10.1371/journal.pone.0013701.

- Vidaurre, D., Arenas, A.L., Smith, S.M., Woolrich, M.W., 2019. Behavioural relevance of spontaneous, transient brain network interactions in fMRI. bioRxiv. https://doi.org/1 0.1101/779736.
- Woolrich, M.W., Jbabdi, S., Patenaude, B., Chappell, M., Makni, S., Behrens, T., Beckmann, C., Jenkinson, M., Smith, S.M., 2009. Bayesian analysis of neuroimaging data in FSL. Neuroimage 45. https://doi.org/10.1016/j.neuroimage.2008.10.055.
- Xu, J., Moeller, S., Auerbach, E.J., Strupp, J., Smith, S.M., Feinberg, D.A., Yacoub, E., Uğurbil, K., 2013. Evaluation of slice accelerations using multiband echo planar imaging at 3T. Neuroimage 83, 991–1001. https://doi.org/10.1016/ j.neuroimage.2013.07.055.
- Yeo, B.T.T., Krienen, F.M., Sepulcre, J., Sabuncu, M.R., Lashkari, D., Hollinshead, M., Roffman, J.L., Smoller, J.W., Zöllei, L., Polimeni, J.R., Fischl, B., Liu, H., Buckner, R.L., 2011. The organization of the human cerebral cortex estimated by intrinsic functional connectivity. J. Neurophysiol. 106, 1125–1165. https://doi.org/ 10.1152/jn.00338.2011.
- Zalesky, A., Fornito, A., Cocchi, L., Gollo, L.L., van den Heuvel, M.P., Breakspear, M., 2016. Connectome sensitivity or specificity: which is more important? Neuroimage 142, 407–420. https://doi.org/10.1016/j.neuroimage.2016.06.035.
- Zanesco, A.P., King, B.G., MacLean, K.A., Jacobs, T.L., Aichele, S.R., Wallace, B.A., Smallwood, J., Schooler, J.W., Saron, C.D., 2016. Meditation training influences mind wandering and mindless reading. Psychol. Conscious. Theory, Res. Pract. 3, 12–33. https://doi.org/10.1037/cns0000082.